International Journal of Geographical Information Science

ISSN: 1365-8816 (Print) 1362-3087 (Online) Journal homepage: http://www.tandfonline.com/loi/tgis20

# Coupling mobile phone and social media data: a new approach to understanding urban functions and diurnal patterns

Wei Tu , Jinzhou Cao, Yang Yue, Shih-Lung Shaw, Meng Zhou , Zhensheng Wang, Xiaomeng Chang, Yang Xu & Qingquan Li

**To cite this article:** Wei Tu , Jinzhou Cao, Yang Yue, Shih-Lung Shaw, Meng Zhou , Zhensheng Wang, Xiaomeng Chang, Yang Xu & Qingquan Li (2017): Coupling mobile phone and social media data: a new approach to understanding urban functions and diurnal patterns, International Journal of Geographical Information Science, DOI: 10.1080/13658816.2017.1356464

**To link to this article:** http://dx.doi.org/10.1080/13658816.2017.1356464

Published online: 31 Jul 2017.

INTERNATIONAL JOURNAL OF GEOGRAPHICAL INFORMATION SCIENCE, 2017
https://doi.org/10.1080/13658816.2017.1356464

ARTICLE

# Coupling mobile phone and social media data: a new approach to understanding urban functions and diurnal patterns

Wei Tu[a,c], Jinzhou Cao[b], Yang Yue[a,c], Shih-Lung Shaw[d], Meng Zhou[a,c,e], Zhensheng Wang[a,c], Xiaomeng Chang[a,c], Yang Xu[f] and Qingquan Li[a,b,c]

[a]Shenzhen Key Laboratory of Spatial Information Smart Sensing and Services, School of Architecture and Urban Planning & Research Institute for Smart Cities, Shenzhen University, Shenzhen, China; [b]State Key Laboratory of Information Engineering in Surveying, Mapping, and Remote Sensing, Wuhan University, Wuhan, China; [c]Key Laboratory for Geo-Environmental Monitoring of Coastal Zone of the National Administration of Surveying, Mapping and GeoInformation, Shenzhen University, Shenzhen, China; [d]Department of Geography, University of Tennessee, Knoxville, TN, USA; [e]Department of Geography, Hong Kong Baptist University, Hong Kong, China; [f]Senseable City Laboratory, SMART Centre, Singapore, Singapore

**ABSTRACT**
Understanding urban functions and their relationships with human activities has great implications for smart and sustainable urban development. In this study, we present a novel approach to uncovering urban functions by aggregating human activities inferred from mobile phone positioning and social media data. First, the homes and workplaces (of travelers) are estimated from mobile phone positioning data to annotate the activities conducted at these locations. The remaining activities (such as shopping, schooling, transportation, recreation and entertainment) are labeled using a hidden Markov model with social knowledge learned from social media check-in data over a lengthy period. By aggregating identified human activities, hourly urban functions are inferred, and the diurnal dynamics of those functions are revealed. An empirical analysis was conducted for the case of Shenzhen, China. The results indicate that the proposed approach can capture citywide dynamics of both human activities and urban functions. It also suggests that although many urban areas have been officially labeled with a single land-use type, they may provide different functions over time depending on the types and range of human activities. The study demonstrates that combining different data on human activities could yield an improved understanding of urban functions, which would benefit short-term urban decision-making and long-term urban policy making.

**ARTICLE HISTORY**
Received 2 January 2017
Accepted 13 July 2017

**KEYWORDS**
Urban function; human activity; mobile phone position data; social media data; data fusion

## 1. Introduction

Urban spaces, where citizens live, move and engage in different activities, are socialized and dynamic. Urban functions are defined as the recognized human uses of urban space, such as residential areas, forests and commercial zones. These functions are important metrics for urban planning and management (Rodrigue *et al.* 2013). However, urban functions are

**CONTACT** Yang Yue yueyang@szu.edu.cn

recognized as macro-static and micro-dynamic (Ratti *et al*. 2006, Batty *et al*. 2012, Zhong *et al*. 2014). From a long-term perspective, urban land is primarily designed to support one type of human activity, e.g. working, shopping, recreation etc. (Liu *et al*. 2012, Crooks *et al*. 2015). In a short-term view, urban land parcels may provide different functions hour by hour, as they actually serve a variety of human activities through the day (Tu *et al*. 2016a). For example, East Asian cities have mixed residential–commercial areas used for housing in the evening but for business during the day. Understanding the detailed diurnal dynamics of these urban functions benefits many urban applications, such as managing traffic congestion, improving public services and promoting smart urban planning (Ahas *et al*., 2015).

Numerous approaches have been developed to monitor urban land use over long time periods. Field observations and interview questionnaires can produce land-use maps, but they are costly and time consuming (Jiang *et al*. 2012). Remote sensing is an alternative methodology for capturing the physical characteristics of land use (Gong and Howarth 1990, Hu and Wang 2013). It relies on the image classification process. Although periodic satellite images, such as those from Landsat and SPOT, have been used to monitor land-use change for some time, some challenges remain. One is the lack of social characteristics of urban land (Pei *et al*. 2014). Commercial zones, educational areas and recreational locations cannot be easily classified from satellite images without additional geographic information. Another challenge is presented by the diurnal dynamic of urban functions. Although many outcomes have been reached by inferring long-term urban land use, it is necessary to investigate urban land's function and diurnal dynamic to more deeply understand daily urban issues. The main challenge is to acquire urban function snapshots that have a high temporal resolution.

In the era of big data, massive human-tracking data that record individuals' positions and times are available (Yue *et al*. 2014, An *et al*. 2015, Li 2017). These include data from mobile phones (Cao *et al*. 2016, Yue *et al*. 2016, Cao *et al*. 2017), social media (Longley *et al*. 2015), vehicle GPS (Tang *et al*. 2016, Tu *et al*. 2016b, Zhou *et al*. 2017) etc. These data contain valuable knowledge about the human use of urban space and therefore provide an alternative approach through which urban function can be inferred. For example, taking mobile phone data as a proxy of human activities, Pei *et al*. (2014) developed a clustering method to classify urban areas by residential, business, commercial, open space and other use. Using social media, trajectory and traffic data, Crooks *et al*. (2015) presented a bottom-up approach to infer the functions of buildings, streets and neighborhoods. These advanced studies support the feasibility of uncovering urban function through (big) data and leave a gap between massive human-tracking data and urban diurnal dynamics.

Each type of human-tracking data has its own shortcomings. Mobile phone data suffer from the lack of semantic information (Calabrese *et al*. 2014). Social media data are sparse in space and time (Huang and Wong 2016). Alone, neither of them is able to provide high temporal resolution for urban functions. To accomplish this, multisourced human-tracking data should be fused (Steiger *et al*. 2015). The aim of this article is to reveal urban functions and their diurnal dynamics by combining mobile phone positioning data with social media check-in data. Unlike the indirect land-use inference approach, this method follows a 'data-activity-function' stream to investigate temporally detailed urban functions from the people who define urban spaces by their daily activities. Citywide human activities are first extracted by integrating mobile phone positioning data with social media check-in data. Homes and workplaces are extracted from mobile phone positioning data by simple spatial–temporal rules used to recognize in-home and working activities. Other activities (such as shopping, schooling, transportation, recreation and entertainment) are annotated with an improved hidden Markov model (HMM) that uses social knowledge learned from long-term social media check-in data. By aggregating identified human activities, hourly urban functions are inferred and the diurnal dynamics of those functions are revealed. An experiment in Shenzhen, China, suggests that many urban cells provide different functions at different hours in a day despite their official designation under one type of land use.

The main contributions of this article lie in two aspects. First, a big data-driven framework is developed for understanding urban dynamics, which bridges the gap between raw tracking data, human activities and the diurnal patterns of urban function. The article also sheds lights on the data fusion of multisourced human-tracking data for human and urban studies. Second, urban functions and their diurnal dynamics as defined by human activities are observed for the first time. The results demonstrate that urban functions are not only spatially distributed but also change hour by hour. This dynamic knowledge about a city will benefit urban decision-making processes, such as traffic congestion management, smart urban planning and urban governance.

The remainder of this paper is organized as follows: the next section reviews the related literature in the domain of mobile phone data analysis, social media data analysis and urban dynamics. Section 3 introduces the fundamental design, including the study area and dataset used. Section 4 describes the proposed data fusion approach. Section 5 reports the experiment and the analysis of the results. Finally, we conclude the paper in Section 6.

## 2. Literature review

This section reviews related studies on mobile phone data analysis, social media data analysis and urban dynamics.

### 2.1. *Mobile phone data analysis*

Mobile phone data are generated when phones connect to mobile communication networks. Because of the high penetration rate and carry-on usage of mobile devices, mobile phone data are of great value to human and urban research domains (Chirag and Storpera 2015), such as human mobility (Gonzalez *et al.* 2008, Song *et al.* 2010, Calabrese *et al.* 2013, Chen *et al.* 2016), mobility landscape (Ratti *et al.* 2006) and urban spatial structure (Louail *et al.* 2014).

One strand of research using mobile phone data focuses on human activity (Xu *et al.* 2016). As mobile phones are always at hand, mobile phone data are recognized as good proxies of people's activities (Tranos and Nijkamp 2015). The position and time of implied human activities can be found through massive mobile phone data. Using call detail records (CDRs), Yuan *et al.* (2012) extrapolated travel activities and examined activity space in Harbin, China. Xu *et al.* (2016) identified anchor points (i.e. homes) from mobile phone positioning data and then quantified home-based mobility patterns. These studies yield insights into important aspects of mobile phone data-driven human activities.

However, the absence of semantic content in mobile phone data hampers deeper analysis. Information on types of activities cannot be directly obtained from mobile phone data because of their low spatial resolution (usually more than 200 m). Understanding citywide human activities and the urban dynamics behind them face great challenges. Although many approaches have been developed for trajectory semantic enrichment, i.e. Bayes activity inferences (Gong *et al*. 2016) and transportation segmentation (Shin *et al*. 2015), labeling activity information using mobile phone data is not easy. Recently, combining mobile phone data with urban land-use data, Widhalm *et al*. (2015) developed a probability approach for extracting daily activities (including in-home activities, working, shopping and leisure) from mobile phone data and analyzed citywide activity patterns. Fusing mobile phone data with data from other sources is another promising approach. Diao *et al*. (2016) integrated 4 months of mobile phone data and household travel surveys to infer activity information to support a longitudinal investigation of individual activities in Boston. These studies indicate the promise of mobile phone data for collecting activities citywide.

Another research stream focuses on urban land use. Recognizing the similarity of calling patterns in one type of land use, Pei *et al*. (2014) developed a semi-supervised fuzzy *c*-means clustering method to classify urban land use and achieved a detection rate of 58.03%. Using time series phone call records, Lenormand *et al*. (2015) presented a functional network approach to automatically detect four types of land use (residential, business, logistics/industrial and nightlife). These studies rely on mobile phone data over a lengthy period to measure the similarity of urban space and thus produce a static land-use map. However, a direct linkage between mobile phone data, human activity and urban function dynamics is required. Unlike Diao *et al*. (2016), in this paper, we fused mobile phone positioning data instead of calls, messaging and web-browsing events with social media check-in data to infer citywide human activities. Social activity knowledge was transferred from social media check-in data to potential human activities to enrich semantic information regarding activities. Furthermore, the diurnal patterns of urban functions portrayed by the obtained citywide human activities were explored.

### 2.2. *Social media data analysis*

Social media data are generated when people post, comment or check-in on social networking websites, such as Twitter, Foursquare and Weibo (Steiger *et al*. 2015). Social media data contain a great deal of semantic information, including texts, pictures, voices, check-in records etc. In particular, a large amount of social media data are geo-referenced using location-awareness technologies (e.g. GPS, WiFi localization, Bluetooth localization etc.) and therefore provide important opportunities to research society, demography and cities (Wu *et al*. 2014, Croitoru *et al*. 2015, Crooks *et al*. 2015, Longley *et al*. 2015, Tsou 2015, Zhou *et al*. 2015). However, biases exist in social media data. For example, the penetration and usage of social media are different for various social media user groups. By using well-designed data filters, long-term social media data can reduce this disadvantage (Longley *et al*. 2015). Social media data are still able to capture aggregated patterns of human activities, especially social activities (Huang and Wong 2016).

Social media data support studies on human social activity. As human behaviors have their own consistency (Gonzalez *et al*. 2008), meaningful places (e.g. office, shopping places and tourism destinations) can be mined from long-term social media data. Combining individual Twitter data and land-use data, Huang *et al*. (2014) developed spatial–temporal clustering methods to infer the locations most visited by individuals on the city-block level and then labeled the daily human activities. Furthermore, based on the home locations, Huang and Wong (2016) inferred the in-home and work activities of social media users. They further linked socioeconomic status and Twitter user groups via urban space by fusing American Community Survey data and Twitter data. Using the 15 million check-in records collected over 1 year in Shanghai, China, Wu *et al*. (2014) extracted citywide transition activities (or travel demands) and investigated the law of related human movements. These studies verified the valuable knowledge about human social activities behind massive social media data.

Social media data also have the potential to infer urban land use (Crooks *et al*. 2015). By considering the similarity of tweeting activities in urban regions, Frías-Martnez and Frías-Martnez (2014) developed an unsupervised learning method to automatically differentiate land uses (including business, residential, night life, leisure, weekend and industrial) in urban areas. Zhan *et al*. (2014) presented an unsupervised clustering method and a supervised learning method to infer urban land use by utilizing a large amount of social media check-in data. Zhou and Zhang (2016) mined Twitter and Foursquare data to extract six types of human activities and detected activity hotspots and their citywide dynamics. These achievements reveal the hidden linkage between human activity patterns and underlying urban form (Crooks *et al*. 2015). They also provide an alternative approach to capture static land use. However, dynamic patterns of urban functions should be further investigated. Furthermore, by combining social media data with other source data, such as data from geographic information system (GIS), mobile phones and travel surveys, more detailed urban function information can be mined from social media content, which can facilitate human and urban research (Steiger *et al*. 2015).



### 2.3. *Urban dynamics*

Urban dynamics refers to human movements and activities over space and time, as reflected in spatial interactions and changes in urban spatial structure through time (Batty 2009, 2010, Grinberger and Shoval 2015). Human activities play an important role in the manifestation of urban dynamics. Recently, the proliferation of spatial–temporal data through technology such as mobile phone data and social media data has opened a new horizon in understanding human movements and activities in space and time.

Spatial dynamics of human activity and land use in cities have been studied (Tranos and Nijkamp 2015). Using long-term CDRs, spatial variations in the intensity of collective human activities have been observed (Sagl *et al*. 2014). Reades *et al*. (2009) proposed an eigen-decomposition method to identify recurring patterns of mobile phone usage and then bridge the relationship between them with residential and business areas. From the temporal view, MIT SENSable City Lab portrayed the urban mobility landscape using massive anonymous mobile phone data (Ratti *et al*. 2006). The intensity of human activities and their changes across space and time were explored. Zhong *et al*. (2014) used 3-year smart card data to reveal the yearly dynamic in the spatial structure of city hubs, centers and borders in Singapore. These studies address the feasibility of the discovery of urban function dynamics but fail to fill a diurnal pattern gap.

Recently, Ahas *et al*. (2015) detected spatial and temporal differences in everyday activities in cities. Following the aggregated rhythm, social time (the time use difference) from human activities was delineated instead of the standard solar time. Their results suggest global temporal dynamics in people's daily lives that cannot be ignored. They also imply that urban lands have different functions at different hours. In this study, we move forward to investigate urban functions and their diurnal dynamics via collective human activities by coupling mobile phone data and social media data. This will enhance our understanding of human activities in the city and the associated urban functions and diurnal patterns.

## 3. Study area and dataset

### 3.1. *Study area*

Shenzhen is China's first special economic zone with a resident population of 12 million and a mobile population of 4 million as of 2012. Its total area covers 1996 square kilometers (Shenzhen Statistical Yearbook 2013). It has six administrative districts, shown in Figure 1. South Shenzhen, adjacent to Hong Kong, contains the downtown (Futian and Luhu) and high-technology zones (Nanshan). North Shenzhen, including Baoan and northern Longgang, is a developing area with factories, lakes and farms. East Shenzhen, including Yantian and eastern Longgang, has an international port and a natural reserve area with country parks and beaches.

### 3.2. *Dataset*

A mobile phone positioning dataset is provided by a major Shenzhen cellular operator that has approximately 5689 cell towers in the city. The dataset contains the positions of 9.2 million phone users (approximately 57.5% of the total population) for a workday in March 2012. The positions of mobile phone users were recorded at half-hour intervals; thus, there are 48 records for each person. Each record has four fields, including a user ID


Figure 1. Shenzhen and its six administrative districts.

**Table 1.** Examples of mobile phone positioning data (the position is marked for privacy).

| User ID | Longitude | Latitude | Time (hh:mm:ss) |
|---|---|---|---|
| 110103203112413 | 113.93* | 22.52* | 07:25:00 |
| 110103203112413 | 113.88* | 22.57* | 07:55:00 |
| 110103203112413 | 113.88* | 22.57* | 08:26:00 |
| 110103203112413 | 113.88* | 22.57* | 08:56:00 |
| – | – | – | – |
| 110103203112413 | 113.93* | 22.52* | 23:28:00 |

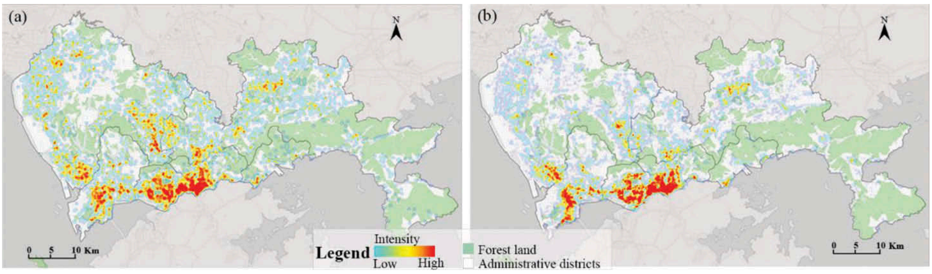


**Figure 2.** Distribution of human-tracking data. (a) Mobile phone positioning data and (b) Sina Weibo check-in data.

($i$), a time stamp ($t$), longitude ($x_{it}$) and latitude ($y_{it}$). Spatial resolution is restricted at the cell tower level, which is approximately 100–500 m. Table 1 shows an example of an individual's records. One row is a positioning record, and no semantic information can be directly obtained. Figure 2(a) illustrates the distribution of records. Following Xu's approach (Xu *et al.* 2016), we divided the study area into a 500-m grid. Ultimately, 2498 grid cells (624.5 km$^2$) contain at least one cell tower, covering 73.3% of the built-up area (851 km$^2$) (China City Statistical Yearbook 2013).

The social media dataset in this study includes check-in records reporting people's activities at points-of-intersects (POIs) with a time stamp (Table 2). It provides semantically rich information about human activities in the city, as the POI suggests what people do in a particular place. The dataset was crawled from Weibo, the largest microblog service provider in China with an open application programming interface (API), and covered the year 2013. Similar to Longley *et al.* (2015), three data filters were applied to avoid shortcomings in the social media check-in data. (1) Users with more than 1000 records in a year are not used. (2) Users with less than three records in a year are omitted. (3) Only two consecutive check-in records with an interval of 1–12 h were used. Finally, 5680,724 check-in records from approximately 520,000 Sina Weibo users were collected and stored in a geodatabase for further processing. Figure 2(b) displays the distribution of Sina Weibo check-in records. It should be noted that we aggregated this dataset to the same grids used for mobile phone positioning data, which suggests that

**Table 2.** Examples of social media check-in data (the position is marked for privacy).

| User ID | Longitude | Latitude | Time | Check-in places |
|---|---|---|---|---|
| 75500001 | 113.93* | 22.52* | 28/3/2013 09:30:00 | Vanke city park |
| 7550042 | 113.78* | 22.43* | 15/4/2013 16:55:00 | Tencent |
| – | – | – | – | – |
| 7557746 | 113.73* | 22.54* | 22/11/2013 23:18:00 | Queen club |

the data have a similar spatial distribution; the density of mobile phone data and social check-in records are generally higher in the southern part of Shenzhen.

In addition to the abovementioned data, additional GIS datasets, including locations of cell towers, spatial data about water and forests etc., are also used in this study.

## 4. Methodology

The presented approach infers urban functions and their diurnal dynamics by fusing massive mobile phone positioning data and social media check-in data. Following a 'data → activity → function' logic, citywide human activities are first extracted, and urban functions are then discovered. Before the introduction of the detailed methodology, some useful definitions are given.

**Definition 1:** *Activities* denote the common activities associated with any person in a day (Zhong *et al*. 2014), such as housekeeping, working and other social actions to meet human needs. To define an activity $a$, six tuples are necessary, including user ID ($i$), start time ($ts_i$), duration ($td_i$), longitude ($x_i$), latitude ($y_i$) and activity type ($a_i$).

To filter out meaningless activities, the duration must be above a threshold, $td_{\mathrm{min}}$. In this study, we set 1 h because the time granularity of mobile phone positioning data is 30 min. In other words, at least three sequential mobile phone records are needed to verify a possible activity in a place. This is reasonable because the durations of common human activities (e.g. in-home, working, schooling etc.) are more than 1 h.

**Definition 2:** *Social activities* refer to nonhome and nonwork activities for human needs. In this research examining social media check-in data, five daily social activities are considered, i.e. $\boldsymbol{S} = \{a_{transportation}, a_{schooling}, a_{shopping}, a_{recreation}, a_{entertainment}\}$, where $\boldsymbol{A_S}$ denotes the set of social activities.

Here, we must note that transportation activity does not refer to travel within the city but rather to air travel, railway travel and long-distance travel by bus. Recreation denotes leisure activities in outdoor places, such as parks and beaches. Entertainment refers to leisure in indoor spaces, e.g. game centers, bars etc. We label social activity from mobile phone positioning data with the knowledge discovered from social media check-in data.

**Definition 3:** *Urban functions* denote people's common usage of urban space, which include residential, working, commercial or educational functions. Generally, urban functions are labeled the dominant human activities in the geographical space.

A data fusion framework is presented to discover urban functions by extracting citywide human activities and labeling functions with them, as Figure 3 illustrates. Potential human activities are first detected from highly penetrated time-sequential mobile phone positioning data. In-home and working activities are recognized using temporal rules. Then, by incorporating learned knowledge from long-term social media check-in data, the remaining social activities are labeled with an improved HMM. After that, a geodatabase containing citywide human activities is built. Finally, urban functions

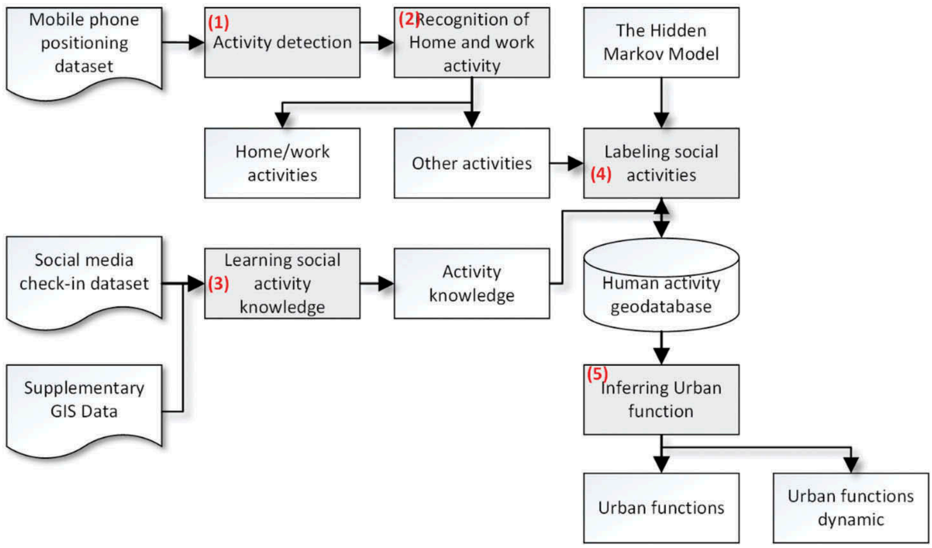


**Figure 3.** The analytical framework of the presented approach.

are inferred from aggregated local human activities, and the diurnal dynamics are analyzed using hourly urban functions.

### 4.1. *Activity detection*

Activity detection extracts potential activities from massive time-sequential mobile phone positioning data. Mobile phone records of an individual are first sorted by time and connected as a spatial–temporal trajectory (Figure 4(a)). Then, if two consecutive records are at the same location, in other words, the person does not move, a potential activity is found, such as $p_1$–$p_2$, $p_6$–$p_7$, $p_9$–$p_{11}$ in Figure 4(b).

Spatial uncertainty exists in mobile phone positioning data because of the low spatial accuracy of cell-tower-based location technology. Consecutive records will jump between adjacent cell towers ($p_3$ in Figure 4(a–c)). Hence, potential activities could be fragmented and shortened. To overcome this shortcoming, a threshold $d$ is used to filter false moves: if the distance from the current point to the previous location is less than $d$, the move can be omitted and the current point can be merged into previous potential points of activity. As Figure 4(c) shows, the record $p_3$ can be merged into previous potential activity ($p_1$–$p_2$). After processing all mobile phone positioning data person by person, a citywide database of potential human activities without type information is constructed.

### 4.2. *Recognition of home and work activities*

In-home activities and working are two main daily behaviors of adult human beings (Schneider *et al.* 2013). The regularity of mobile phone positioning data indicates information on homes and workplace (Xu *et al.* 2016). Considering the rhythms of human beings, we label a person’s in-home and working activities using the following rules.

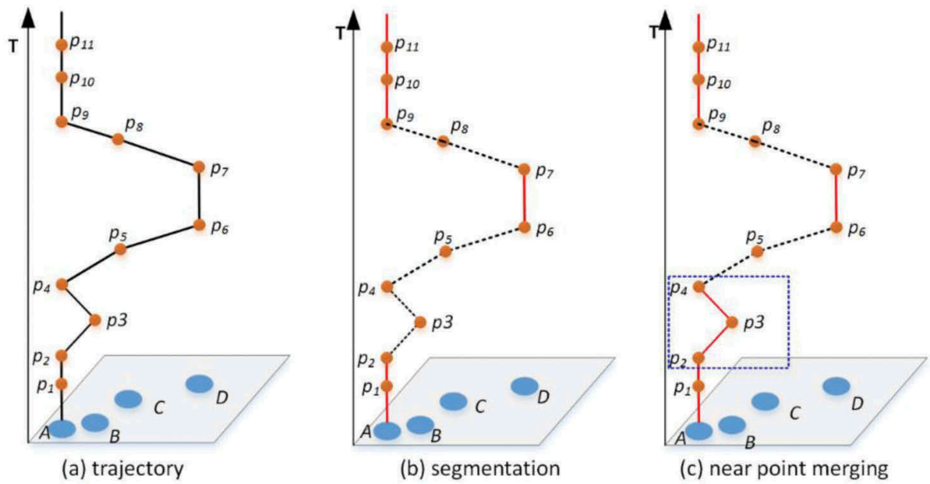


**Figure 4.** Activity detection with mobile phone positioning data.

- **Home rule**: For an individual, if the total duration in a place occupies more than half of the early morning period [0:00–6:00], this place will be defined as home. All activities located at the home of this person are defined as in-home activities.
- **Workplace rule**: If the total duration in a place occupies more than half of the daily working period [9:00–12:00] and [14:00–17:00], this place will be defined as the workplace. All activities located in the workplace of this person are defined as working activities.

In total, we labeled the homes of 91.9% of mobile users and the workplaces of 64.8% of users and therefore annotated 75.7% of the potential activities.

### 4.3. *Learning social activity knowledge from social media data*

Social media check-in data contain the spatial–temporal characteristics of human activities. Within the timeline of social media check-in data, the transition between activities is also implied. We mined the social media check-in data of 1 year to gain knowledge about social activities. First, Weibo check-in data are labeled as one type of activity according to their checked POIs in Table 3. Then, following the check-in sequence of Weibo users, the probability of daily activity transition was generated. Figure 5 displays the distance and interval distribution of the consecutive potential human activities described in Section 4.1 and those of the Sina Weibo check-in data. This figure indicates that both datasets show a similar decay pattern except at the 2-h interval. Therefore, it is reasonable to transfer social activities knowledge from Sina Weibo check-in data to mobile phone positioning data. Table 4 reports the daily activity transition matrix, which seems skewed toward social activities. As 75.8% of potential activities were labeled in-home and working, this information is helpful for annotating the remaining activity.

The normal daily activity transition matrix has been refined in space and time to improve knowledge about social activity. By considering the spatial heterogeneity of human

**Table 3.** Labeling for social media check-in information types.

| Check-in POIs | Activity type |
|---|---|
| Home, residential locations | In-home |
| Office building, government, company, industrial park, hospital, bank, post office | Working |
| Shopping mall, supermarket, store | Shopping |
| Airport, railway station, long-distance bus station, customs ports | Transportation |
| University, primary school, high school, scientific research institution, library | Schooling |
| Park, gym, beach, soccer field, zoo, museum, scenic spots | Recreation |
| Chinese/Western restaurant, tea room, coffee shop, diner, nightclub, pub, bar, theater, beauty salon, Karaoke, bath massage, Internet bar, arcade, temple | Entertainment |

POI: Points-of-intersects.

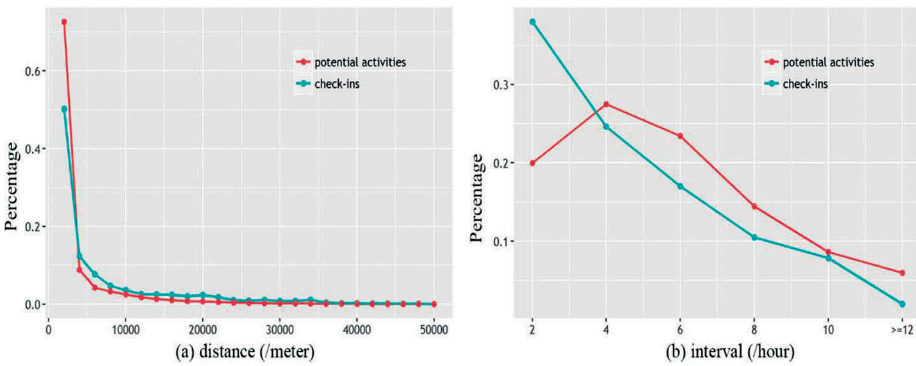


**Figure 5.** Distribution of potential human activities and consecutive Sina Weibo check-in data.

activities, we discovered the spatial-dependent activity transition matrix (Figure 6). According to the location of POI, the number of a type of activity $a$ in a grid cell $i$, $N_a^i$, is calculated. Following an individual's timeline, the number of transitions between two types of activities (activity $a$ to activity $b$) and from one place to another ($i$–$j$), $N_{ab}^{ij}$, is also calculated. By dividing $N_a^i$ by the total number of activities in grid $i$, $\sum_{a\in A} N_a^i$, the generation probability of one type of activity $a$ at grid $i$, $p(a|i)$, is calculated as Equation (1). By dividing $N_{ab}^{ij}$ by the total number of activity transitions between grid $i$ and $j$, $N_{ab}^{ij}$, the transition probability between activities, $p(ab|ij)$, is also calculated as Equation (2).

$$p(a|i) = \frac{N_a^i}{\sum_{a\in A} N_a^i} \tag{1}$$

**Table 4.** Daily activity transition matrix from social media data.

| Activity | | In-home | Working | Shopping | Transportation | Schooling | Recreation | Entertainment |
|---|---|---|---|---|---|---|---|---|
| | | Second activity | | | | | | |
| First activity | In-home | 0.20 | 0.16 | 0.15 | 0.11 | 0.11 | 0.12 | 0.14 |
| | Working | 0.16 | 0.18 | 0.14 | 0.13 | 0.12 | 0.13 | 0.14 |
| | Shopping | 0.15 | 0.13 | 0.18 | 0.11 | 0.09 | 0.13 | 0.16 |
| | Transportation | 0.11 | 0.14 | 0.13 | 0.31 | 0.09 | 0.14 | 0.11 |
| | Schooling | 0.13 | 0.15 | 0.12 | 0.11 | 0.42 | 0.14 | 0.12 |
| | Recreation | 0.12 | 0.13 | 0.14 | 0.13 | 0.10 | 0.22 | 0.13 |
| | Entertainment | 0.14 | 0.12 | 0.15 | 0.11 | 0.08 | 0.12 | 0.21 |

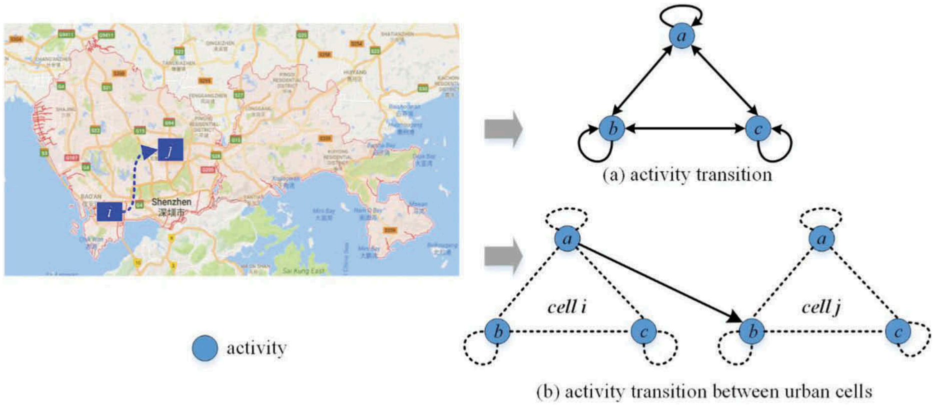


**Figure 6.** Learning activity knowledge from social media data (a, b, c denote types of activities).

$$p(ab|ij) = \frac{N_{ab}^{ij}}{\sum_{a \in A, b \in A} N_{ab}^{ij}} \tag{2}$$

Considering the temporal rhythm of human activities, we divided the day into three intervals $T1$ = [0:00–6:00), $T2$ = [6:00–17:00), $T3$ = [17:00–24:00). Then, the time-dependent activity transition probabilities were calculated as Equation (3), where $p$, $q$ denotes an interval, and $p$ is no later than $q$. Thus, a spatial–temporal activity transition matrix was generated and used later for social activity labeling.

$$p(ab|ijpq) = \frac{N_{ab}^{ijpq}}{\sum_{a \in A, b \in A} N_{ab}^{ijpq}} \tag{3}$$

### 4.4. *Labeling social activities with the HMM*

The HMM could recognize unobserved (hidden) states from observed states (Rabiner 1989, Eddy 2004). We used the HMM to infer information about the remaining activity types based on prior knowledge of in-home and work activities (in Section 4.2) and the spatial–temporal activity transition knowledge from social media check-in data (in Section 4.3).

In the HMM, each unobserved state is associated with a probability distribution. Transitions among the hidden states are fit with a set of transition probabilities. In a specific state, an observation can be generated by the associated probability distribution. However, the hidden state is not directly observable to an external observer. Formally, there are five components in the HMM, HMM $= \{H, O, A, B, \pi\}$.

- $= (h_1, h_2, \ldots, h_N)$ is the set of hidden states and $N$ is the number of hidden states in the model. Here, we denote activities as hidden states.
- $O = (o_1, o_2, \ldots, o_M)$ is the set of observations and $M$ is the number of distinct observation symbols per state. In this study, we denote the activity locations as the observation $O$. Therefore, $M$ is the number of distinct grids.
- $A = \{a_{ij}\}$ is the state transition probability distribution, $a_{ij} = p_r\{a_{t+1} = S_j | a_t = S_i\}$, $1 \leq i, j \leq N$, where $a_t$ refers to the state at time $t$.

- $B = \{b_i(k)\}$ is the observation probability distribution in each of the states, $b_i(k) = p_r\{v_k \, at \, t | q_t = S_j\}$, $1 \le j \le N$, $1 \le k \le M$.
- $\pi = \{\pi_i\}$ is the initial state distribution, $\pi_i = p_r\{q_1 = S_i\}$, $1 \le i \le N$.

Therefore, for a series of observations, $O = (o_1, o_2, \ldots, o_T)$ at time $T$, where each observation $o_i \in T$, $1 \le i \le T$, the HMM finds the most likely hidden state sequence $Q = (q_1, q_2, \ldots, q_T)$, where $q_i \in H$, $1 \le i \le T$.

Figure 7 presents the adoption of the HMM for social activity labeling. The hidden states refer to the activity set. The observation refers to the activity location. The transition between hidden states corresponds to the transition between consecutive activities as a person moves in the city. The observation probability denotes the spatial distribution of a type of activity. The initial state is a person's first activity in a day. When the first potential activity is detected as an in-home or working, the initial state is known. Otherwise, it is randomly selected from the activity set and determined by the following *Viterbi* algorithm.

The *Viterbi* algorithm (Viterbi 1967) is used to search the most likely activity sequence $A = (a_1, a_2, \ldots, a_T)$ for a given sequence of potential activity in Section 4.1. A *Viterbi* variable is defined as

$$\gamma_{t+1}(j) = \left[\max_i \gamma_t(i) \cdot a_{ij}\right] \cdot b_j(O_{t+1}), \quad 1 \le t \le T \tag{4}$$

where $\gamma_t(i)$ is the highest probability along a single potential activity sequence at state t, $a_{ij}$ is the state transition probability from $i$ to $j$, and $b_j(O_{t+1})$ is the observation probability at state $j$. To obtain the most likely social activity, $\mu_{t+1}(j)$ is defined as

$$\gamma_{t+1}(j) = \operatorname{argmax}\left(\gamma_t(i) \cdot a_{ij}\right), \quad 1 \le t \le T \tag{5}$$

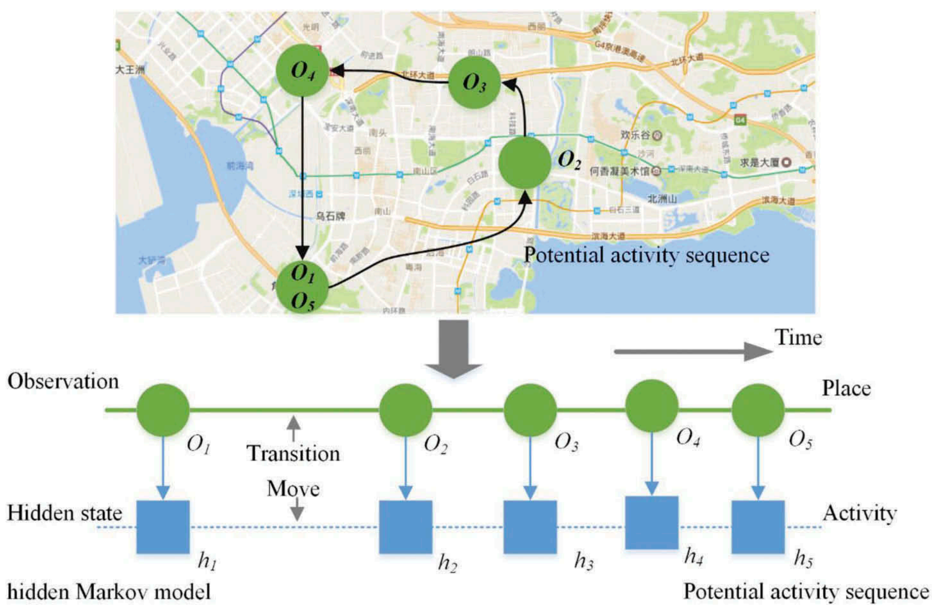


**Figure 7.** Labeling social activities in the hidden Markov model.

It should be noted that the ordinary HMM must be improved for the variations in human activities. The probability of Equation (4) and (5) approaches the spatial–temporal activity transition identified in Section 4.3 such that the temporal fluctuation effect of human activity can be alleviated, and the obtained human activities are more reliable.

### 4.5. *Inferring urban functions*

Using citywide human activities, the functions of each urban cell can be inferred. First, the proportions of seven types of activities are calculated as variables to characterize urban cells. The proportion of one activity $p_a$ in a cell is calculated as Equation (6), where $N_a$ is the percentage of a type of activity $a$ and $A$ is the activity set. Then, urban cells are classified with a hierarchical cluster analysis (Smith and Dubes 1980). Next, according to the average proportions of the seven types of activities, we set the urban cells' urban functions, including the residential function (RF), industrial function (IF), commercial function (CF), educational function (EDF), transportation function (TF), recreational function (REF), entertainment function (ENF) and mixed function (MF), with the dominant activity. Using hourly human activity information, spatial–temporal high-resolution urban functions are obtained, allowing their diurnal dynamics to be analyzed. To investigate the change in the diversity of urban functions, their entropies are calculated in Equation (7), where $p_i$ is the percentage of urban functions $i$ and $F$ is the function set.

$$p_a = \frac{N_a}{\sum_{a \in A} N_a} \tag{6}$$

$$E = \sum_{i \in F} -p_i \log p_i \tag{7}$$

## 5. Results and analysis

Massive mobile phone positioning data and Sina Weibo check-in data in Section 3 were combined by using a developed program with the Arc Engine 10.3 application programming interface. Urban functions were inferred with the help of the citywide human activities database. This section reports the results of human activities and the diurnal dynamics of urban functions.

### 5.1. *Human activities*

In total, 31,669,042 activities were contributed by 9.2 million persons in Shenzhen after fusing mobile phone positioning data and Sina Weibo check-in data. On average, one person conducts 3.41 activities in a day. Table 5 reports the summary of human activities. In-home and working activities are the main daily human activities in the city. There are 14,470,460 in-home activities and 10,459,657 working activities, which account for approximately 45.7% and 33.0% of total activities, respectively. Social activities constitute the small remainder. The most frequent social activity is entertainment (2408,597, approximately 7.6% of daily activities), while the least frequent social activity is schooling (872,231, approximately 2.8% of daily activities).

**Table 5.** Summary of daily activities in Shenzhen, China.

| | | | Social activity | | | | |
|---|---|---|---|---|---|---|---|
| Activities | In-home | Working | Transportation | Schooling | Shopping | Recreation | Entertainment |
| Number | 14,470,460 | 10,459,657 | 1228,703 | 872,231 | 1428,106 | 801,288 | 2408,597 |
| Ratio | 45.7% | 33.0% | 3.9% | 2.8% | 4.5% | 2.5% | 7.6% |
| Ratio in Shenzhen household travel survey 2010 | 42.85% | 34.32% | 2.96% | 4.79% | 4.13% | 2.52% | – |

The activity results were first validated using the available population data. A correlation analysis has been conducted for in-home activities at night and the population within the traffic analysis zone reported by the Shenzhen Yearbook 2013. The Pearson correlation coefficient is 0.92, which indicates that the analyses are significantly correlated with a confidence level $p = 0.01$. Therefore, the count for in-home activities is credible.

To further validate the results, we compared the activity ratios with those derived from the 2010 Shenzhen household travel survey. The comparison indicates these ratios match well for transportation, shopping and recreation activities, with a gap less than 1.0%. The gap for in-home, working, schooling and entertainment activities appears slightly larger, which could be for following reasons. One is that the travel survey focuses less on the mobile population, which contributes less to schooling but more to working. The second reason is that the travel survey does not investigate entertainment activity. The third reason is that students in primary and middle school are forbidden to access mobile phones. Because their schooling activities are not detected, the identified schooling activity is lower than that obtained in the travel survey.

Citywide human activities have a significant temporal rhythm. Figure 8(a) displays the fluctuation of in-home and working activities. The number of in-home activities reaches its peak of 7.82 million in the early morning (3:00), falls to 2.53 million in the afternoon (15:00) and recovers to near 6.64 million at midnight (23:00). Working activities show a reverse trend, beginning with only 0.54 million in the early morning, rising to a peak at noon (4.47 million at 15:00) and then declining to less than 2.0 million at night.

Social activities also display a typical temporal wave. In total, 6738,923 social activities are conducted each day. As with working activities, social activities begin the lowest in the early morning (0.22 million at 4:00), reach their first peak in the morning (1.05 million at 10:00) and their second peak at night (1.85 million at 21:00), as Figure 7(a) shows. However, social activities display different rhythms. Figure 8(b) shows the fluctuation of all five types of social activities, demonstrating that entertainment activities have two peaks, one at morning (10:00) and the other at night (22:00). Transportation reaches its first maximum in the morning and its second peak value at night. The remaining four social activities have only one peak. Both shopping and recreation reach their peaks at night and fall in the early morning. Schooling is quite low in the early morning and increases in the day.

The composition of activities also varies with the time of day. Figure 8(c) displays the hourly activity percentages, suggesting that the proportions of in-home and working activities are larger than 75% at any time of day. Social activities account for approximately 12% of the morning and afternoon. However, they account for 21% at 20:00 and reach their peak at 21:00. This fluctuation suggests different functions provided by urban land at different times of day.

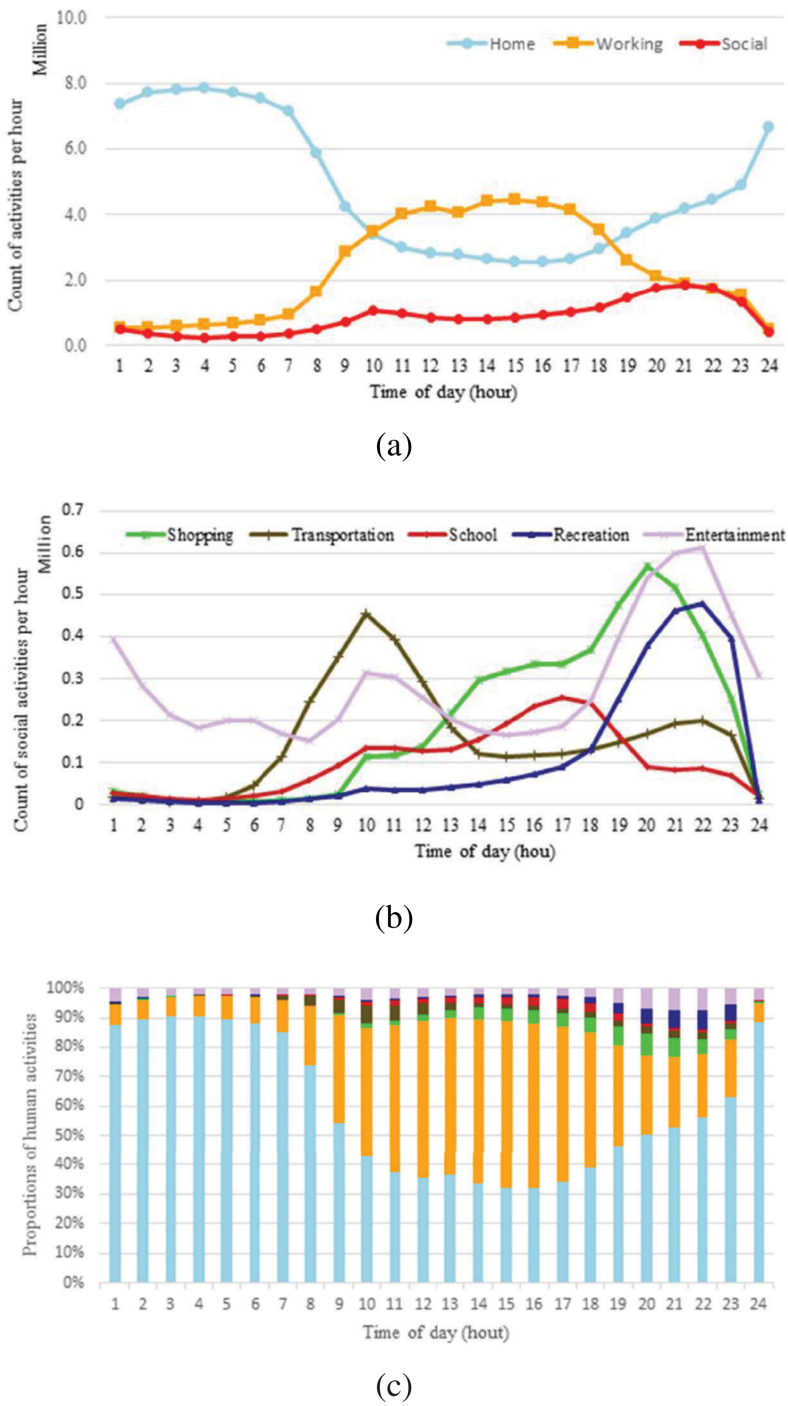


**Figure 8.** The fluctuation of daily human activities. (a) Human activity per hour, (b) social activity per hour and (c) the proportions of human activities throughout the day.

Figure 9 shows the spatial distribution of human activities. In-home activities are widely distributed in the city (Figure 9(a)), appearing in many urban cells and spatially aggregating in many places, such as downtown and western and central Shenzhen. Unlike in-home activities, working activities occur with the highest density in the downtown area, which is the central business district with many tall buildings (Figure 9(b)). The density of working activities declines from south to north, although northern Shenzhen is an industrial area with low-floor factories and farms. Five types of social activities are also scattered through the city but occur relatively less frequently in most spatial cells, occurring at a high density in only few cells. For example, cells with high-density shopping activities are located where there are shopping centers (Figure 9(c)).

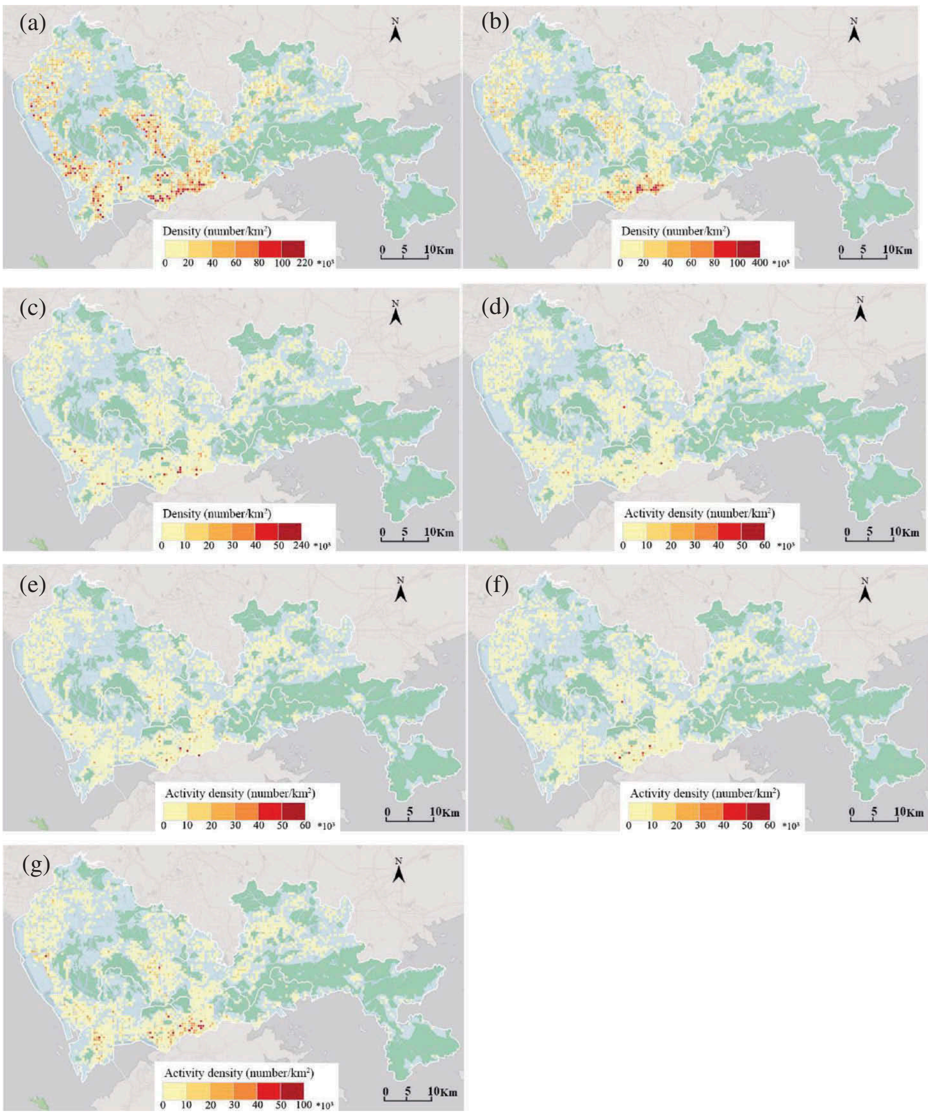


**Figure 9.** Spatial distribution of human activities: (a) In-home, (b) working, (c) shopping, (d) schooling, (e) transportation, (f) recreation and (g) entertainment.

Cells of high-density schooling activities have universities and technology institutes, among others (Figure 9(d)). This distribution suggests an even urban function distribution.

## 5.2. Urban function dynamics

### 5.2.1. Results for urban functions

Using daily human activity information, 2498 urban cells are classified into 8 clusters using the proportions of human activities, as described in Section 4.5. Ultimately, eight types of clusters are obtained. Table 6 describes the average proportions of human activities in each cluster. By comparing the global mean proportion of human activity, we classified urban cells into eight functions: RFs with 0.501 in-home activities; IFs with 0.501 working activities; CFs with 0.251 shopping activities, TFs with 0.211 transportation activities; EDFs with 0.176 schooling activities; REFs with 0.244 recreation activities; ENF with 0.318 entertainment activities and MF with 0.211 in-home, 0.374 working and 0.415 social activities. This indicates that most human activities are mixed in all types of urban functional cells because of their fragmented use in this city.

Table 7 reports the summary of urban cells with functions and demonstrates that RF and IF are the main functions provided by this city. Many cells feature RF (1438 cells) and IF (409 cells), as in-home and working activities are the main activities in this city. Social functions compose an important part of urban functions. A few cells feature TF (183), EF (152) or REF (112), and fewer than 100 cells feature CF (94) or ENF (78); the fewest cells feature MF (32). Although there are fewer schooling activities than shopping and entertainment activities, there are more EDF cells than CF and ENF cells because schooling activities are distributed in universities and schools, which occupy large spaces. However, most commercial activities occur in stores along the roads in Shenzhen, while entertainment activities occur at restaurants and clubs, which are usually small and therefore can be found within residential or IFs.

Figure 10 displays the distribution of urban functions and illustrates that cells with RF are spatially adjacent, forming a few neighborhoods, such as the residential areas in Nanshan, Baoan and Longgang. IF cells are also grouped at the center of Nanshan, the center of Futian, the west part of Baoan and the port of Hong Kong. The remaining six types of urban functions are sparsely scattered throughout the city, surrounding RF and IF areas.

### 5.2.2. Comparison with land zoning map

Inferred urban functions were compared with the official Shenzhen land zoning map (2010–2020) from the Shenzhen Urban Planning, Lands and Resource Commission to evaluate the obtained results. In total, 58% of urban cells have the same urban function and designed land use, similar to the results of Pei *et al.* (2014) in Singapore. Table 8 presents the confusion matrix between land use and daily urban functions. It illustrates that RF, IF, CF and EDF present a consistent accuracy level of no less than 50%, while TF, REF, ENF and MF present a consistent accuracy level below 50%, which implies differences between the land zoning map and real urban functions in Shenzhen, China. There are two possible reasons for these differences. One is that some urban cells have changed their functions, following the human usage of urban cells. In fact, Shenzhen is the fastest developing city in China. The usage of land parcels changes greatly. For

**Table 6.** The mean proportion of human activities of different urban functions.

| Urban functions | In-home | Working | Shopping | Transportation | Schooling | Recreation | Entertainment |
|---|---|---|---|---|---|---|---|
| Global mean | **0.436** | **0.341** | **0.043** | **0.046** | **0.031** | **0.030** | **0.074** |
| RF | **0.501** | 0.310 | 0.038 | 0.031 | 0.021 | 0.022 | 0.077 |
| IF | 0.279 | **0.501** | 0.046 | 0.053 | 0.031 | 0.026 | 0.064 |
| CF | 0.357 | 0.324 | **0.251** | 0.012 | 0.011 | 0.003 | 0.041 |
| TF | 0.452 | 0.283 | 0.011 | **0.211** | 0.009 | 0.004 | 0.031 |
| EDF | 0.464 | 0.296 | 0.014 | 0.006 | **0.176** | 0.018 | 0.026 |
| REF | 0.379 | 0.297 | 0.006 | 0.024 | 0.012 | **0.244** | 0.038 |
| ENF | 0.271 | 0.338 | 0.026 | 0.011 | 0.016 | 0.021 | **0.318** |
| MF | 0.211 | 0.374 | 0.110 | 0.080 | 0.044 | 0.085 | 0.095 |

RF: Residential functions; IF: industrial functions; CF: commercial functions; TF: transportation functions; EDF: education functions; ENF: entertainment functions; MF: mixed functions. The bold texts indicate the proportion more than the global mean.

**Table 7.** Characteristics of urban functions.

| Functions | RF | IF | CF | TF | EDF | REF | ENF | MF |
|---|---|---|---|---|---|---|---|---|
| Number of cells | 1438 | 409 | 94 | 183 | 152 | 112 | 78 | 32 |
| Ratio | 57.6% | 16.4% | 3.8% | 7.3% | 6.1% | 4.5% | 3.1% | 1.3% |

RF: Residential functions; IF: industrial functions; CF: commercial functions; TF: transportation functions; EDF: education functions; ENF: entertainment functions; MF: mixed functions; REF: Recreational functions.

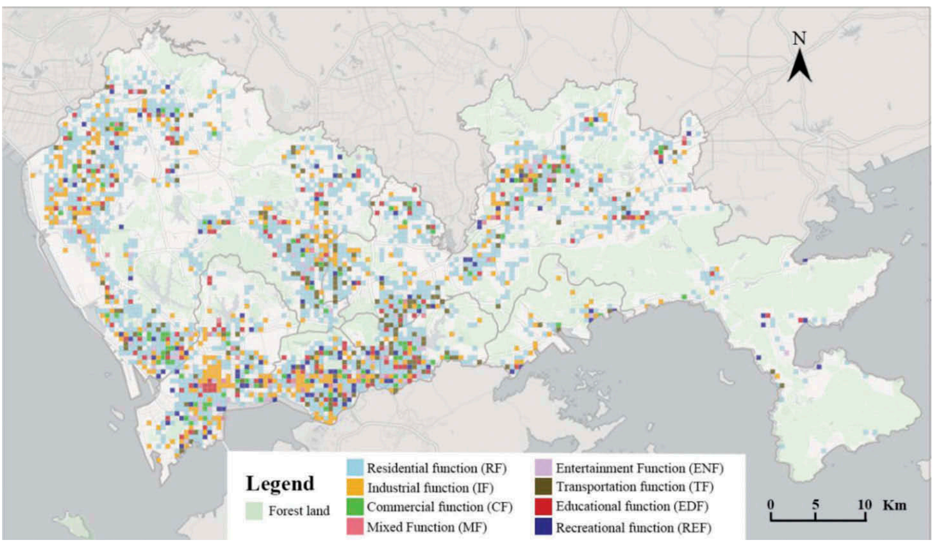


**Figure 10.** Distribution of urban functions in Shenzhen.

example, many old factories in south Shenzhen have been changed to residential buildings or commercial parks as a result of urban renewal. The other reason for differences is because function is measured for each urban cell, as land parcels are substantially fragmented and used for different purposes. Aggregating human activities to make urban function inferences may generate errors.

### 5.2.3. *Dynamics of urban functions*

Using the proportions of human activities per hour, high temporal resolution urban functions were inferred. Figure 11 displays the change in urban functions provided by

**Table 8.** The comparison of urban functions with land use.

| Functions | | Official land-use map | | | | | | | |
|---|---|---|---|---|---|---|---|---|---|
| | | RF (%) | IF (%) | CF (%) | TF (%) | EDF (%) | REF (%) | ENF (%) | MF (%) |
| This study | RF | **58** | 15 | 10 | 4 | 5 | 3 | 3 | 1 |
| | IF | 17 | **61** | 5 | 5 | 5 | 3 | 4 | 1 |
| | CF | 14 | 19 | **50** | 2 | 7 | 2 | 4 | 1 |
| | TF | 4 | 21 | 12 | **46** | 7 | 2 | 7 | 1 |
| | EDF | 18 | 12 | 7 | 1 | **51** | 3 | 7 | 1 |
| | REF | 5 | 16 | 15 | 4 | 6 | **46** | 6 | 0 |
| | ENF | 9 | 24 | 13 | 4 | 6 | 3 | **41** | 0 |
| | MF | 25 | 9 | 13 | 6 | 0 | 6 | 3 | **38** |

RF: Residential functions; IF: industrial functions; CF: commercial functions; TF: transportation functions; EDF: education functions; ENF: entertainment functions; MF: mixed functions; REF: Recreational functions. The bold value indicates the ratio of the same function.



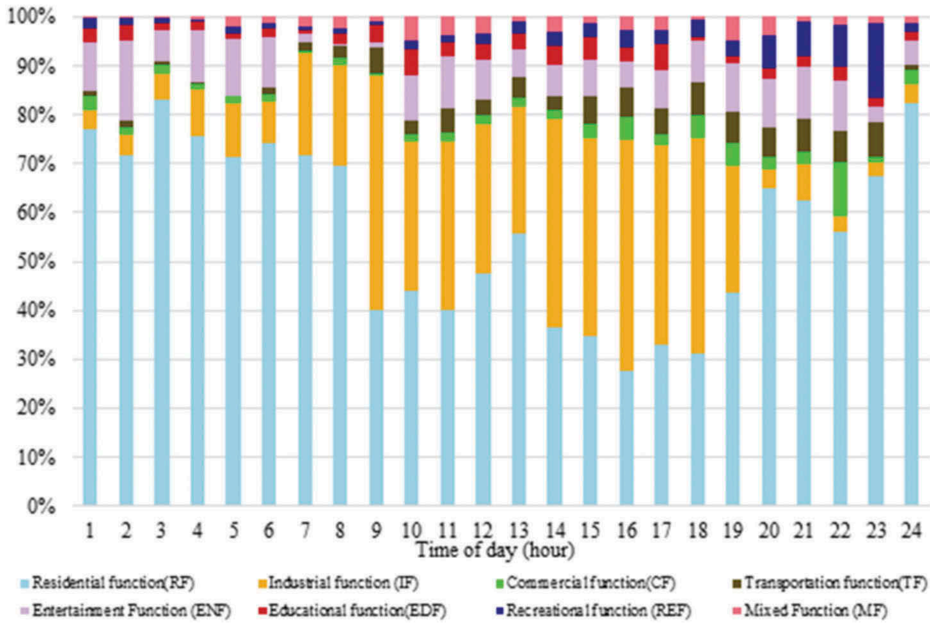


**Figure 11.** The rhythm of urban functions in Shenzhen, China.

the city and shows that urban functions are quite different at different times of day. Following the rhythms of human activities, the RF begins at a high percentage (approximately 75%), falls in the morning, increases at noon, falls again in the afternoon and finally recovers at night. The IF shows an almost reverse trend. It begins with a low percentage (less than 10%), increases in the morning and declines at night. The remaining six types of functions also vary with human activity rhythms. The percentage of EDF is low at night but high during the day, reaching peaks at 10:00 and 17:00. The MF is almost nonexistent at night but occupies approximately 2–5% of total cells during the day. However, REF is more frequent at night and in the afternoon but less so in the morning, which may be a result of the lower value of other social activities, as Figure 10 shows.

Taking four places as examples, we examined the reliability of the inferred human activities and the associated urban function dynamic. Figure 12(a) displays the result of Yingrenshi village, a residential community. It illustrates that this cell has 8000 in-home activities during the night while about 2000 in the day; therefore, its function is dominated by the RF in the whole day. Figure 12(b) reports the observed activities in and the hourly function of Shenzhen North high-speed railway station. This figure indicates that human activities increase from night to day in this place, but transportation activity rises very sharply, arriving the peak 2452 at 10 h, which is in accordance with the schedule of high-speed railway. This activity diurnal dynamic leads to a transformation from the RF to transportation. Figure 12(c) illustrates the activities and function dynamic at a cell near Shenzhen University. The schooling and the working activities rise significantly in this cell, which supports the highest school 2854 activities (per cell) during the day; these functions are labeled educational in this time period. Workplaces in the central business district are indicated in Figure 12(d), which displays the change in in-home, working, recreation and entertainment activities. It indicates that the working activities are no more than 200 in the night and arrive the peak 7952 at 14 h and reduce to the fewest 100 in the night. The associated function transforms from

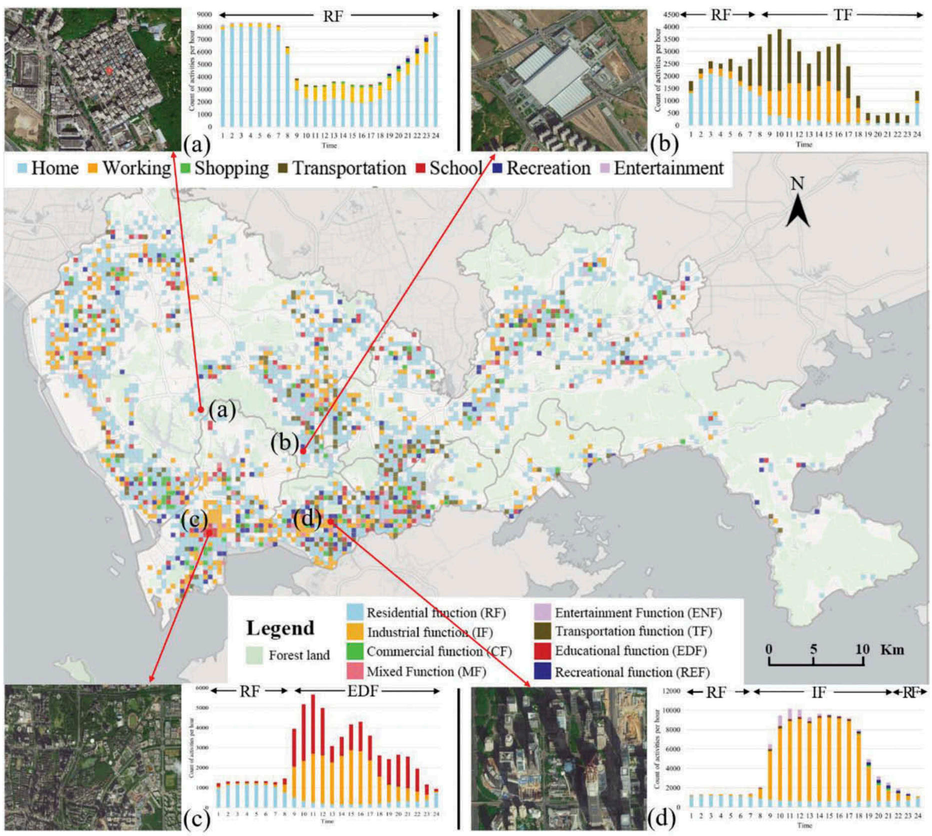


**Figure 12.** The functions of four places: (a) a residential community, (b) Shenzhen North high-speed railway station, (c) Shenzhen University and (d) residential–working mixed area.

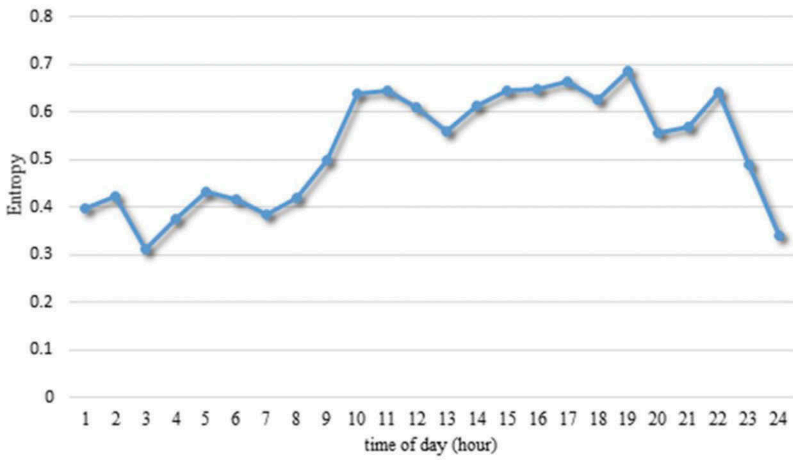


**Figure 13.** The entropy of urban functions in Shenzhen, China.



residential to industrial and back to residential. In summary, both activity and function results in these places suggest the effectiveness of the proposed data fusion approach.

Figure 13 displays the entropy of urban functions, which illustrates that the entropy is quite low and that diversity is quite low at night, as the main provided function is for residential purposes. In the daytime, the entropy increases as the diversity of urban functions rises. The maximum entropy occurs in the 19:00 h, which indicates that the city provides the greatest variety of functions. Then, entropy begins to decline as people go back to their homes and the city returns to being a residential space.

To further investigate the diurnal dynamics of urban functions, the function transitions at the same cell in typical time periods are analyzed. Figure 14 shows the observed transitions between hourly urban functions and suggests that many cells change from RF to IF and MF in the period [7:00–10:00] as people leave their homes for work. Therefore, RFs provided by urban land are weakened, but both IFs and MFs are strengthened.

In the afternoon period [15:00–18:00] when people are off duty and return home, many cells with IFs change to provide RFs (Figure 15). However, half of the cells still represent IFs, as work continues until 20:00. The number of ENF cells increases because many entertainment venues, such as bars and clubs, open at that time. MF urban cells also increase as people conduct quite different activities after work.

With respect to the night period (22:00–1:00), many people have returned home. Accordingly, the number of cells with non-RFs (including IFs, TFs, recreation functions and ENFs) declines, but the number of cells with RFs significantly increases (Figure 16). Notably, there are still a few cells with IFs, as some factories operate on three shifts for 24 h.

## 6. Discussion and conclusion

The city is a complex system of human activities and their interactions with space and its associated dynamics. Understanding urban functions and their dynamics is essential for the planning, managing and governing of a city. Understanding how urban functions

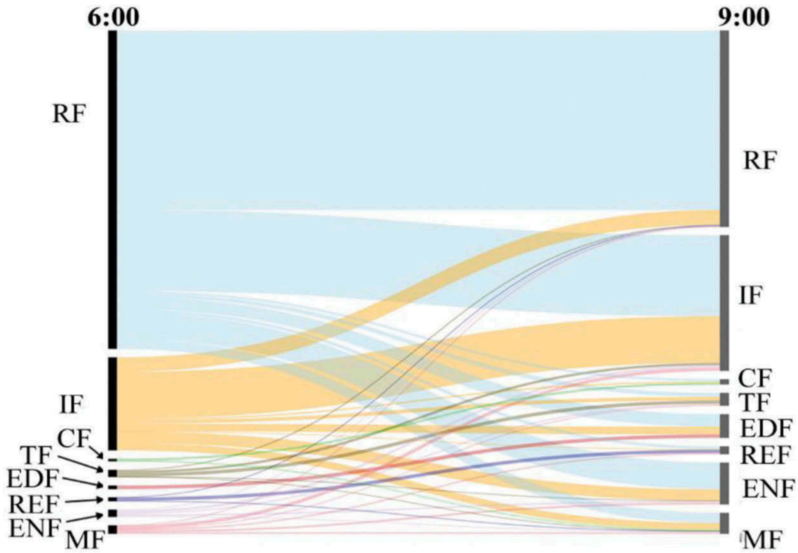


**Figure 14.** The change in urban functions from 7:00 to 10:00.

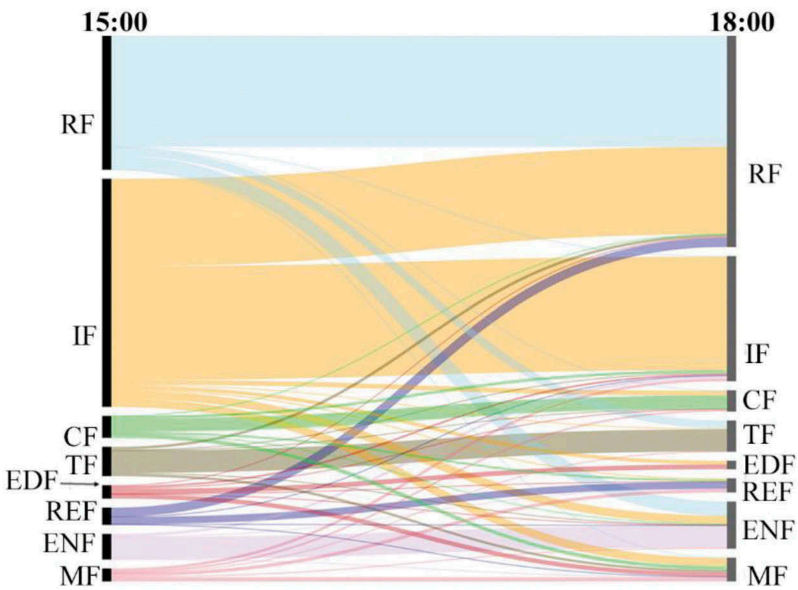


**Figure 15.** The change in urban functions from 15:00 to 18:00.

vary across space and time is very challenging. In the era of big data, massive human-tracking data are available (e.g. mobile phone data, GPS data, social media data etc.) and open a new horizon for urban function inference. However, a single type of human-tracking data has its own drawbacks. For example, mobile phone data lack semantic information, while social media data are sparse in space and time. Multisourced human-tracking data should be fused to discover urban function dynamics.

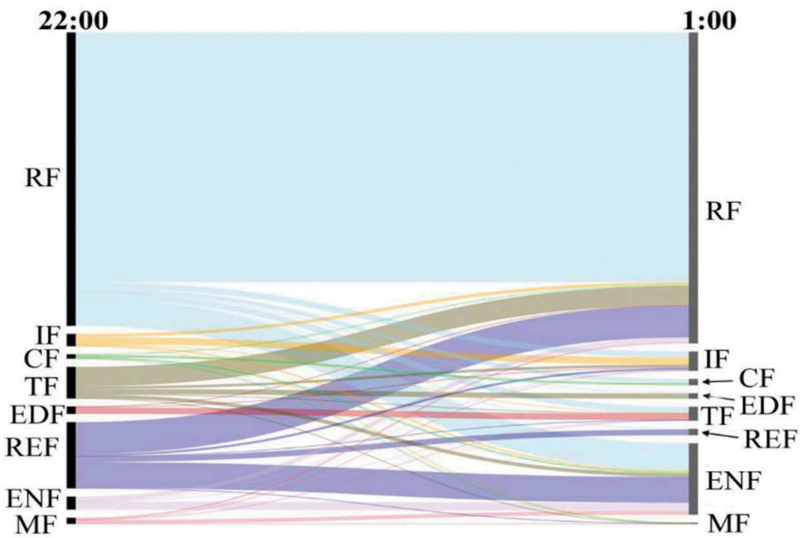


**Figure 16.** The change in urban functions from 22:00 to 1:00.



Following a ‘data-activity-function’ philosophy, this article develops a data fusion approach to uncover urban functions and their diurnal dynamics by coupling mobile phone positioning data and social media data. Citywide detailed spatial–temporal human activities are first recovered from multisourced spatial–temporal data. In-home and working activities are identified from massive mobile phone positioning data. The remaining five social activities are annotated with their type information (such as travel, schooling, shopping, recreation and entertainment) by the HMM inference with the knowledge learned from social media check-in data. Then, the percentage of human activities in each urban cell is calculated. By clustering spatial cells with similar compositions of human activities, urban functions are recognized. Their hourly dynamics are analyzed with the obtained spatial–temporal high-resolution human activity data.

The experiment was conducted in Shenzhen, China. The obtained results demonstrate that both human activities and urban functions change in spatial and temporal dimensions. Urban cells with residential or IFs are clustered in the city. However, urban cells with essential social functions, such as commercial, educational and ENFs, are sparsely scattered throughout the city. Compared to the land-zoning map, 58% of urban cells have the same inferred urban functions, which implies that there are differences between land-use planning and real urban functions in Shenzhen, China.

The results also reveal that urban functions change hour by hour. Following the cycle of human activities, the functions provided by urban cells undergo significant changes among residential, industrial and social functions, and this study presents the first description of this typical diurnal dynamic, providing an image of the transitions of human activities and the associated urban functions, which suggests that although many urban cells have officially been labeled with one type of land use, they may provide different functions at different times of day as they host different human activities.

The proposed study develops an alternative approach to investigating urban functions and massive human-tracking data via human activities. The obtained results bridge the gap between big data, human activity analysis and urban dynamics. They also offer a deeper understanding of urban land, which will benefit short-term urban decision-making, e.g. traffic management and emergency response, among others.

This study has several limitations. First, due to constraints in data availability, mobile phone positioning data in this study were used for only one working day. As many studies have investigated the consistency of human activities based on mobile phone data (Sevtsuk and Ratti 2010, Song *et al.* 2010), we believe that a 1-day mobile phone dataset is feasible to uncover urban function dynamics. The results can be further improved by analyzing mobile phone positioning data over a longer period. Second, due to the sparsity of social media data, a few differences between human activities from mobile phone data and social media data were observed (as Figure 5). Additionally, social media check-in data and mobile phone positioning data were collected in 2014 and 1 day in 2012, respectively. Therefore, biases are inevitably imported into the learned social activity characteristics. In the further, multi-sourced big geographical data, such as POIs, geo-tagged photos and travel survey data, should be integrated to enrich the knowledge obtained from social media check-in data. The reliability of human activities and, subsequently, urban functions may be improved. Third, as a pioneering work regarding citywide human activities, the reliability of the results was not directly examined. Alternative approaches to harvesting high-resolution spatial and temporal data on citywide human activities are expected.

## Acknowledgments

We would like to thank three anonymous reviewers for their valuable comments on this article.

## Disclosure statement

No potential conflict of interest was reported by the authors.

## Funding

This work was supported by the National Natural Science Foundation of China: [Grant Numbers 41401444, 41671387 and 91546106]; Shenzhen Scientific Research and Development Funding Program: [Grant Number CXZZ20150504141623042]; Nature Science Foundation of Shenzhen University: [Grant Number 2016065] andthe Open Fund of Key Laboratory of Urban Land Resources Monitoring and Simulation, Ministry of Land and Resources: [Grant Numbers KF-2016-02-009 and KF-2016-02-010].

## ORCID

Wei Tu http://orcid.org/0000-0002-0255-4037
Meng Zhou http://orcid.org/0000-0001-5172-9967

## References


Ahas, R., *et al*., 2015. Everyday space–time geographies: using mobile phone-based sensor data to monitor urban activity in Harbin, Paris, and Tallinn. *International Journal of Geographical Information Science*, 29 (11), 2017–2039. doi:10.1080/13658816.2015.1063151

An, L., *et al*., 2015. Space–time analysis: concepts, quantitative methods, and future directions. *Annals of the Association of American Geographers*, 105 (5), 891–914. doi:10.1080/00045608.2015.1064510

Batty, M., 2010. The pulse of the city. *Environment and Planning B: Planning and Design*, 37 (4), 575–577. doi:10.1068/b3704ed

Batty, M., *et al*., 2012. Smart cities of the future. *The European Physical Journal Special Topics*, 214, 481–518. doi:10.1140/epjst/e2012-01703-3

Batty, M., 2009. Urban modeling. *In*: R. Kitchin and N. Thrift, eds. *International encyclopedia of human geography*. Oxford: Elsevier.

Calabrese, F., *et al*., 2013. Understanding individual mobility patterns from urban sensing data: a mobile phone trace example. *Transportation Research Part C: Emerging Technologies*, 26, 301–313. doi:10.1016/j.trc.2012.09.009

Calabrese, F., Ferrari, L., and Blondel, V.D., 2014. Urban sensing using mobile phone network data: a survey of research. *ACM Computing Surveys*, 47 (2), 1–20. doi:10.1145/2658850

Cao, J., *et al*., 2017. Spatio-temporal analysis of aggregated human activities based on massive mobile phone tracking data. *Journal of Geo-Information Science*, 19 (4), 467–474.

Cao, R., *et al*., 2016. Comparison of urban human movements inferring from multi-source spatial-temporal data. *Intentional archive of photogrammetry and remote sensing, and spatial information science*, XLI-B2, 471–476.

Chen, C., *et al*., 2016. The promises of big data and small data for travel behavior (aka human mobility) analysis. *Transportation Research Part C: Emerging Technologies*, 68, 285–299. doi:10.1016/j.trc.2016.04.005

China City Statistical Yearbook, 2013. Beijing: *China statistical press*.

Chirag, R. and Storpera, M., 2015. The digital skin of cities urban theory and research in the age of the sensored and metered city, ubiquitous computing and big data. *Cambridge Journal of Regions, Economy and Society*, 25 (1), 27–42.

Croitoru, A., *et al*., 2015. Linking cyber and physical spaces through community detection and clustering in social media feeds. *Computers Environment and Urban Systems*, 53, 47–64. doi:10.1016/j.compenvurbsys.2014.11.002

Crooks, A., *et al*., 2015. Crowdsourcing urban form and function. *International Journal of Geographical Information Science*, 29 (5), 720–741. doi:10.1080/13658816.2014.977905

Diao, M., *et al*., 2016. Inferring individual daily activities from mobile phone traces: a Boston example. *Environment and Planning B: Planning and Design*, 43 (5), 920–940. doi:10.1177/0265813515600896

Eddy, S.R., 2004. What is a hidden Markov model? *Nature Biotechnology*, 22 (10), 1315–1316. doi:10.1038/nbt1004-1315

Frías-Martnez, V. and Frías-Martnez, E., 2014. Spectral clustering for sensing urban land use using Twitter activity. *Engineering Application of Artificial Intelligence*, 35, 237–245. doi:10.1016/j.engappai.2014.06.019

Gong, L., *et al*., 2016. Inferring trip purposes and uncovering travel patterns from taxi trajectory data. *Cartography and Geographic Information Science*, 43 (2), 103–114. doi:10.1080/15230406.2015.1014424

Gong, P. and Howarth, P., 1990. The use of structural information for improving land-cover classification accuracies at the rural-urban fringe. *Photogrammetric Engineering and Remote Sensing*, 56 (1), 67–73.

Gonzalez, M.C., Hidalgo, C.A., and Barabasi, A.L., 2008. Understanding individual human mobility patterns. *Nature*, 453 (7196), 779–782. doi:10.1038/nature06958

Grinberger, A.Y. and Shoval, N., 2015. A temporal-contextual analysis of urban dynamics using location-based data. *International Journal of Geographical Information Science*, 29 (11), 1969–1987. doi:10.1080/13658816.2015.1049951

Hu, S.G. and Wang, L., 2013. Automated urban land-use classification with remote sensing. *International Journal of Remote Sensing*, 34 (3), 790–803. doi:10.1080/01431161.2012.714510

Huang, Q., Cao, G., and Wang, C., 2014. From where do tweets originate?: a GIS approach for user location inference. *ACM SIGSpatial International Workshop on Location-Based Social Networks,* Nov 2014, Dallas, Texas, USA. New York: ACM, 1–8.

Huang, Q. and Wong, D.W.S., 2016. Activity patterns, socioeconomic status and urban spatial structure: what can social media data tell us? *International Journal of Geographical Information Science*, 30 (9), 1873–1898. doi:10.1080/13658816.2016.1145225

Jiang, S., Ferreira, J., and Gonzalez, M.C., 2012. Clustering daily patterns of human activities in the city. *Data Mining and Knowledge Discovery*, 25 (3), 478–510. doi:10.1007/s10618-012-0264-z

Lenormand, M., *et al*., 2015. Comparing and modelling land use organization in cities. *Royal Society Open Science*, 2 (12), 150449. doi:10.1098/rsos.150449

Li, Q., 2017. From geomatics to urban informatics. *Geomatics and Information Science of Wuhan University*, 42 (1), 1–6.

Liu, Y., *et al*., 2012. Urban land uses and traffic 'source-sink areas': evidence from GPS-enabled taxi data in Shanghai. *Landscape and Urban Planning*, 106 (1), 73–87. doi:10.1016/j.landurbplan.2012.02.012

Longley, P.A., Adnan, M., and Lansley, G., 2015. The geotemporal demographics of twitter usage. *Environment and Planning A*, 47 (2), 465–484. doi:10.1068/a130122p

Louail, T., *et al*., 2014. From mobile phone data to the spatial structure of cities. *Scientific Reports*, 4, 5276. doi:10.1038/srep05276

Pei, T., *et al*., 2014. A new insight into land use classification based on aggregated mobile phone data. *International Journal of Geographical Information Science*, 28 (9), 1988–2007. doi:10.1080/13658816.2014.913794

Rabiner, L.R., 1989. A tutorial on hidden Markov models and selected applications in speech recognition. *Proceedings of the IEEE*, 77 (2), 257–286. doi:10.1109/5.18626

Ratti, C., *et al*., 2006. Mobile landscapes: using location data from cell phones for urban analysis. *Environment and Planning B: Planning and Design*, 33 (5), 727–748. doi:10.1068/b32047

Reades, J., Calabrese, F., and Ratti, C., 2009. Eigenplaces: analysing cities using the space-time structure of the mobile phone network. *Environment and Planning B: Planning and Design*, 36 (5), 824–836. doi:10.1068/b34133t

Rodrigue, J.-P., Comtois, C., and Slack, B., 2013. *The geography of transport systems*. London: Routledge.

Sagl, G., Delmelle, E., and Delmelle, E., 2014. Mapping collective human activity in an urban environment based on mobile phone data. *Cartography and Geographic Information Science*, 41 (3), 272–285. doi:10.1080/15230406.2014.888958

Schneider, C.M., *et al*., 2013. Unravelling daily human mobility motifs. *Journal of the Royal Society Interface*, 10 (84), 20130246. doi:10.1098/rsif.2013.0246

Sevtsuk, A. and Ratti, C., 2010. Does urban mobility have a daily routine? Learning from the aggregate data of mobile networks. *Journal of Urban Technology*, 17 (1), 41–60. doi:10.1080/10630731003597322

Shenzhen Statistical Yearbook, 2013. Shenzhen Statistical Yearbook. Available from: http://www.sztj.gov.cn/nj2013/start%202013.htm. [Accessed 13 October 2016].

Shin, D., *et al*., 2015. Urban sensing: using smartphones for transportation mode classification. *Computers, Environment and Urban Systems*, 53, 76–86. doi:10.1016/j.compenvurbsys.2014.07.011

Smith, S.P. and Dubes, R., 1980. Stability of a hierarchical clustering. *Pattern Recognition*, 12 (3), 177–187. doi:10.1016/0031-3203(80)90042-4

Song, C., *et al*., 2010. Limits of predictability in human mobility. *Science*, 327 (5968), 1018–1021. doi:10.1126/science.1177170

Steiger, E., De Albuquerque, J.P., and Zipf, A., 2015. An advanced systematic literature review on spatiotemporal analyses of twitter data. *Transactions in GIS*, 19 (6), 809–834. doi:10.1111/tgis.12132

Tang, L.L., *et al.*, 2016. A network Kernel density estimation for linear features in space–time analysis of big trace data. *International Journal of Geographical Information Science*, 30 (9), 1717–1737. doi:10.1080/13658816.2015.1119279

Tranos, E. and Nijkamp, P., 2015. Mobile phone usage in complex urban systems: a space–time, aggregated human activity study. *Journal of Geographical Systems*, 17 (2), 157–185. doi:10.1007/s10109-015-0211-9

Tsou, M.-H., 2015. Research challenges and opportunities in mapping social media and Big Data. *Cartography and Geographic Information Science*, 42, 70–74. doi:10.1080/15230406.2015.1059251

Tu, W., *et al.*, 2016a. Optimizing the locations of electric taxi charging stations: a spatial–temporal demand coverage approach. *Transportation Research Part C: Emerging Technologies*, 65, 172–189. doi:10.1016/j.trc.2015.10.004

Tu, W., *et al.*, 2016b. Spatial-temporal variation of public transit ridership using smart card data and mobile phone data. *Association of American Geographers Annual Meeting 2016,* April 2016, San Francisco, USA. Washington: AAG.

Viterbi, A., 1967. Error bounds for convolutional codes and an asymptotically optimum decoding algorithm. *IEEE Transactions on Information Theory*, 13 (2), 260–269. doi:10.1109/TIT.1967.1054010

Widhalm, P., *et al.*, 2015. Discovering urban activity patterns in cell phone data. *Transportation*, 42 (4), 597–623. doi:10.1007/s11116-015-9598-x

Wu, L., *et al.*, 2014. Intra-urban human mobility and activity transition: evidence from social media check-in data. *PLoS ONE*, 9 (5), e97010–e97010. doi:10.1371/journal.pone.0097010

Xu, Y., *et al.*, 2016. Another tale of two cities: understanding human activity space using actively tracked cellphone location data. *Annals of the American Association of Geographers*, 106 (2), 489–502.

Yuan, Y., Raubal, M., and Liu, Y., 2012. Correlating mobile phone usage and travel behavior – a case study of Harbin, China. *Computers, Environment and Urban Systems*, 36 (2), 118–130. doi:10.1016/j.compenvurbsys.2011.07.003

Yue, Y., *et al.*, 2014. Zooming into individuals to understand the collective: a review of trajectory-based travel behaviour studies. *Travel Behaviour and Society*, 1 (2), 719–723. doi:10.1016/j.tbs.2013.12.002

Yue, Y., *et al.*, 2016. Measurements of POI-based mixed use and their relationships with neighbourhood vibrancy. *International Journal of Geographical Information Science*, doi:10.1080/13658816.2016.1220561

Zhan, X., Ukkusuri, S.V., and Zhu, F., 2014. Inferring urban land use using large-scale social media check-in data. *Networks and Spatial Economics*, 14 (3–4), 647–667. doi:10.1007/s11067-014-9264-4

Zhong, C., *et al.*, 2014. Detecting the dynamics of urban structure through spatial network analysis. *International Journal of Geographical Information Science*, 28 (11), 2178–2199. doi:10.1080/13658816.2014.914521

Zhou, M., *et al.*, 2015. Inferring individual physical locations with social friendships. *In*: *Proceedings of geoinfomatics 2015*. Wuhan, China: IEEE, 1–6.

Zhou, M., *et al.*, 2017. Impacts of weather on public transport ridership: results from mining data from different sources. *Transportation Research Part C: Emerging Technologies*, 75, 17–29. doi:10.1016/j.trc.2016.12.001

Zhou, X.L. and Zhang, L., 2016. Crowdsourcing functions of the living city from Twitter and Foursquare data. *Cartography and Geographic Information Science*, 43 (5), 393–404. doi:10.1080/15230406.2015.1128852